

Supporting Information for:

High-Coordinate Co^{II} and Fe^{II} compounds Constructed from an Asymmetric Tetradentate Ligand Showing Slow Magnetic Relaxation Behavior†

Xing-Cai Huang,*^a Zi-Yi Qi,^a Chen-Long Ji,^a Yi-Ming Guo,^a Shi-Chang Yan,^a Yi-Quan Zhang,^{*b} Dong Shao^c and Xin-Yi Wang*^c

a School of Chemistry and Environmental Engineering, Yancheng Teachers University, Yancheng, 224007, China. E-mail: huangxc82@126.com.

b Jiangsu Key Laboratory for NSLSCS, School of Physical Science and Technology, Nanjing Normal University, Nanjing 210023, China. E-mail: zhangyiquan@nynu.edu.cn

c State Key Laboratory of Coordination Chemistry, Collaborative Innovation Centre of Advanced Microstructures, School of Chemistry and Chemical Engineering, Nanjing University, Nanjing, 210093, China. E-mail: wangxy66@nju.edu.cn

Dalton Trans.

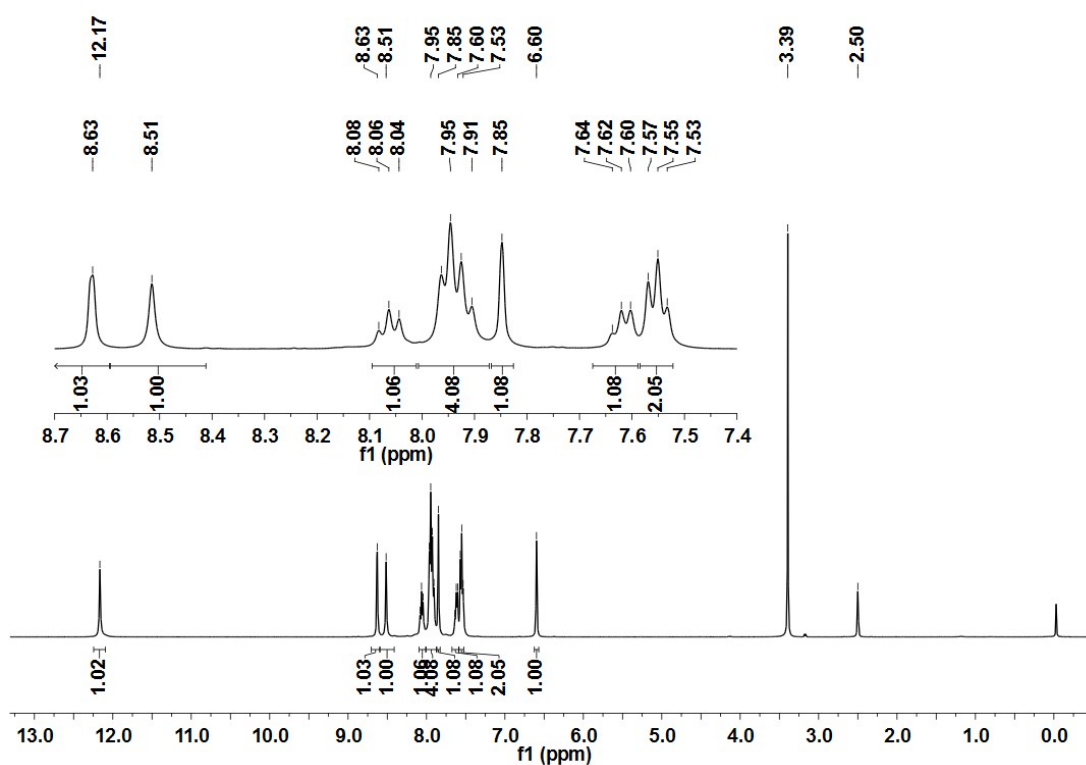


Fig. S1. ^1H NMR spectra of the ligand pypzbeyz at 298K in DMSO-D6

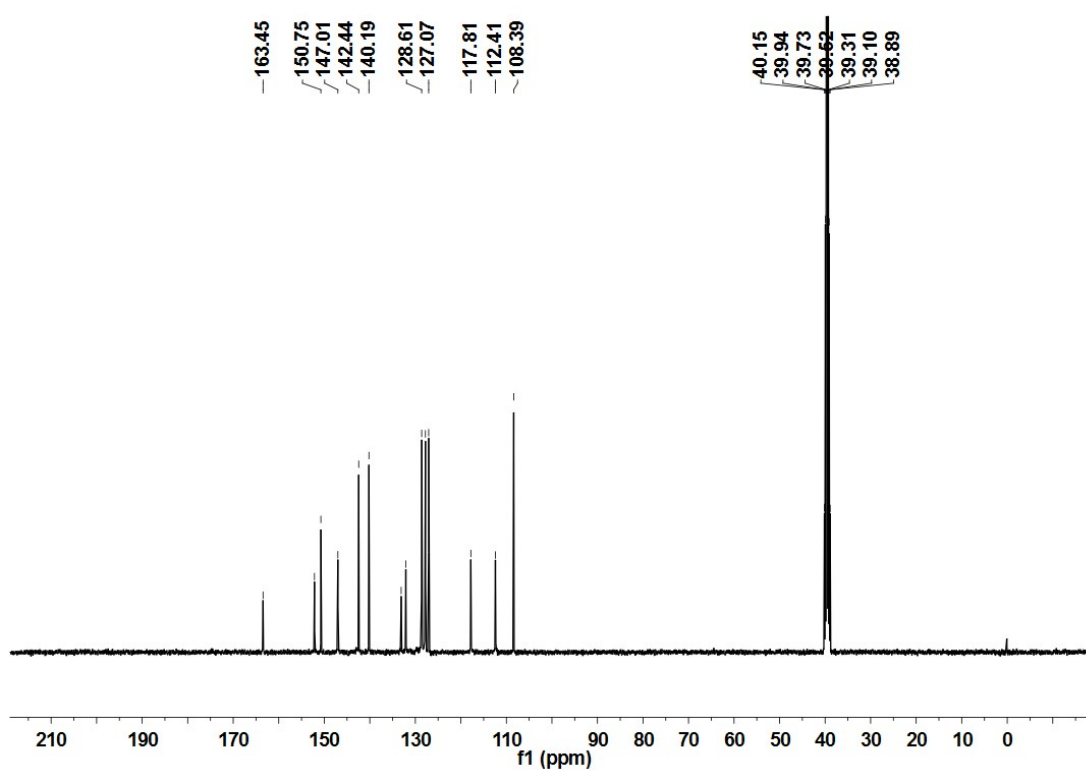


Fig. S2. ^{13}C NMR spectra of the ligand pypzbeyz at 298K in DMSO-D6

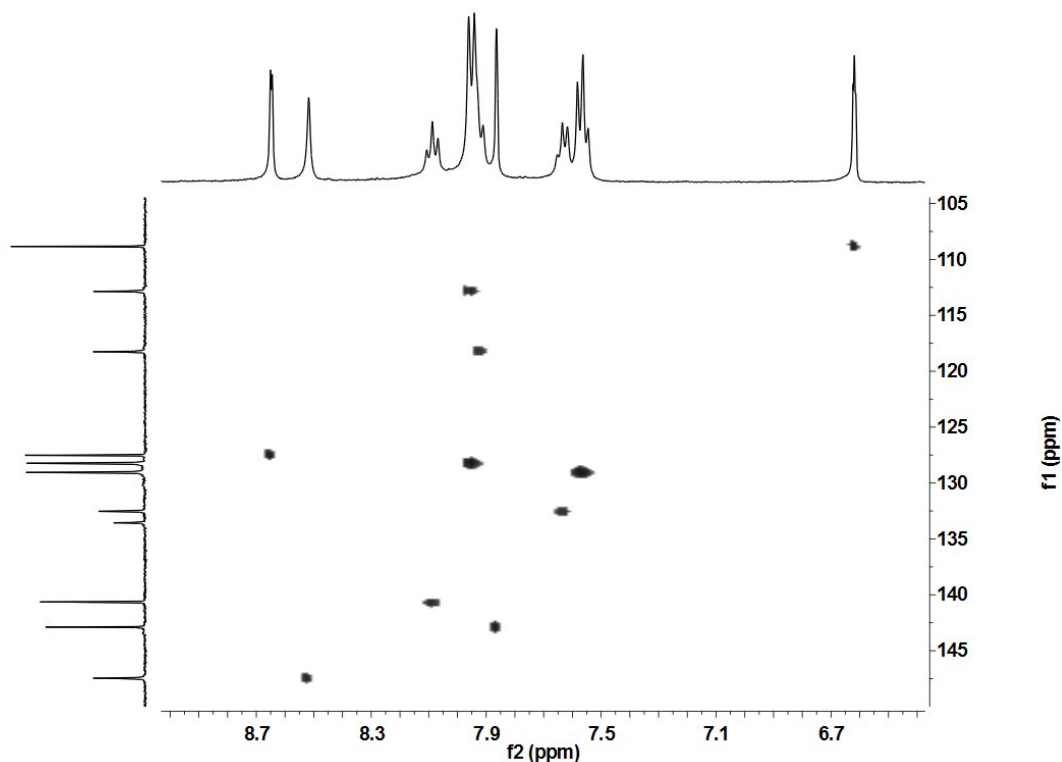


Fig. S3. HSQC and HMBC spectra of the ligand pypzbeyz at 298K in DMSO-D6

Table S1. Selected Bond Distances [Å] and angles [°] for **1** and **2**

1			
Co1-O5	2.0879(19)	Co1-N4	2.1913(19)
Co1-O2	2.1242(19)	Co1-O1	2.2140(17)
Co1-N1	2.1637(19)	Co1-O4	2.241(2)
Co1-N3	2.184(2)	Co1···O6	3.0701(32)
O5-Co1-O2	176.49(5)	O2-Co1-N3	89.74(7)
O5-Co1-N1	88.57(7)	N1-Co1-N3	72.04(7)
O2-Co1-N1	94.54(7)	O5-Co1-N4	87.52(7)
O5-Co1-N3	92.77(8)	O2-Co1-N4	91.97(7)
N1-Co1-N4	70.66(7)	N1-Co1-O1	140.08(6)
N3-Co1-N4	142.68(7)	N3-Co1-O1	146.98(6)
O5-Co1-O1	82.87(7)	N4-Co1-O1	70.08(7)
O2-Co1-O1	93.68(7)	O5-Co1-O4	119.78(7)
O2-Co1-O4	58.33(7)	N4-Co1-O4	131.96(7)
N1-Co1-O4	140.49(6)	O1-Co1-O4	74.91(7)
N3-Co1-O4	79.16(7)		
2			
Fe1-N8	2.243(3)	Fe1-N9	2.305(3)
Fe1-O1	2.255(3)	Fe1-O2	2.310(3)
Fe1-N6	2.278(3)	Fe1-N3	2.323(3)
Fe1-N4	2.298(3)	Fe1-N1	2.327(3)
N8-Fe1-O1	91.21(10)	O1-Fe1-N4	68.78(10)

N8-Fe1-N6	69.87(11)	N6-Fe1-N4	138.76(10)
O1-Fe1-N6	79.37(10)	N8-Fe1-N9	137.78(10)
N8-Fe1-N4	84.92(11)	O1-Fe1-N9	78.99(10)
N6-Fe1-N9	67.98(10)	N6-Fe1-O2	135.14(10)
N4-Fe1-N9	127.10(10)	N4-Fe1-O2	72.12(10)
N8-Fe1-O2	154.64(10)	N9-Fe1-O2	67.21(9)
O1-Fe1-O2	90.38(10)	N8-Fe1-N3	89.60(11)
O1-Fe1-N3	156.45(9)	O2-Fe1-N3	98.83(10)
N6-Fe1-N3	78.83(10)	N8-Fe1-N1	84.22(11)
N4-Fe1-N3	134.69(10)	O1-Fe1-N1	135.60(9)
N9-Fe1-N3	84.66(10)	N6-Fe1-N1	137.74(10)
N4-Fe1-N1	66.83(10)	O2-Fe1-N1	77.05(10)
N9-Fe1-N1	130.54(10)	N3-Fe1-N1	67.88(10)

Table S2. The Co^{II} center of geometry analysis for **1** by SHAPE software

Structure[ML ₇]	HP-7	HPY-7	PBPY-7	COC-7	CTPR-7	JPBPY-7	JETPY-7
1	28.474	22.249	3.010	5.037	3.323	5.934	20.194
HP-7 1 <i>D</i> _{7h} Heptagon; HPY-7 2 <i>C</i> _{6v} Hexagonal pyramid; PBPY-7 3 <i>D</i> _{5h} Pentagonal bipyramid; COC-7 4 <i>C</i> _{3v} Capped octahedron; CTPR-7 5 <i>C</i> _{2v} Capped trigonal prism; JPBPY-7 6 <i>D</i> _{5h} Johnson pentagonal bipyramid J13; JETPY-7 7 <i>C</i> _{3v} Johnson elongated triangular pyramid J7.							

Table S3. The Fe^{II} center of geometry analysis for **1** by SHAPE software

Structure[ML ₈]	OP-8	HPY-8	HBPY-8	CU-8	SAPR-8	TDD-8	JGBF-8
2	31.539	24.240	14.762	12.730	3.753	1.472	11.556
Structure[ML ₈]	JETBPY-8	JBTPR-8	BTPR-8	JSD-8	TT-8	ETBPY-8	
2	26.575	3.136	2.394	2.969	13.391	22.662	
OP-8 1 <i>D</i> _{8h} Octagon; HPY-8 2 <i>C</i> _{7v} Heptagonal pyramid; HBPY-8 3 <i>D</i> _{6h} Hexagonal bipyramid; CU-8 4 <i>O</i> _h Cube; SAPR-8 5 <i>D</i> _{4d} Square antiprism; TDD-8 6 <i>D</i> _{2d} Triangular dodecahedron; JGBF-8 7 <i>D</i> _{2d} Johnson gyrobifastigium J26; JETBPY-8 8 <i>D</i> _{3h} Johnson elongated triangular bipyramid J14; JBTPR-8 9 <i>C</i> _{2v} Biaugmented trigonal prism J50; BTPR-8 10 <i>C</i> _{2v} Biaugmented trigonal prism; JSD-8 11 <i>D</i> _{2d} Snub diphenoid J84; TT-8 12 <i>T</i> _d Triakis tetrahedron; ETBPY-8 13 <i>D</i> _{3h} Elongated trigonal bipyramid							

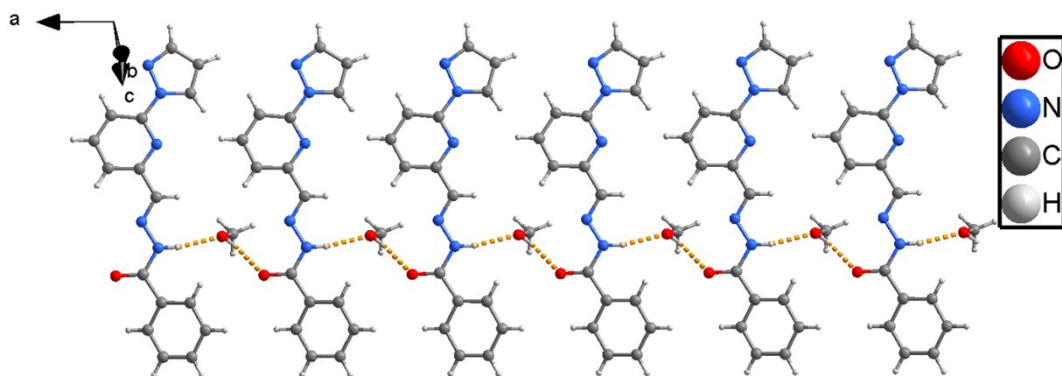


Fig. S4. Hydrogen bonding network in **pypzbeyz·CH₃OH**

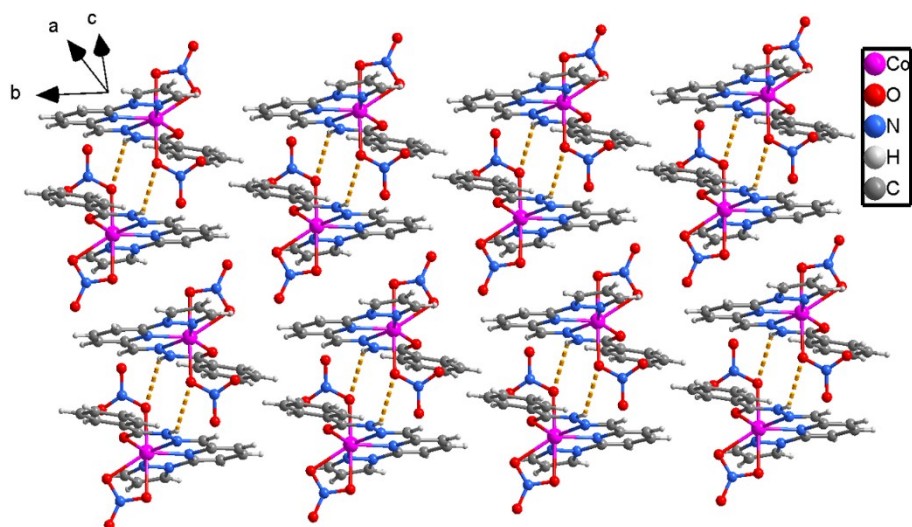


Fig. S5. The π - π packing diagram and hydrogen bonding network in **compound 1**

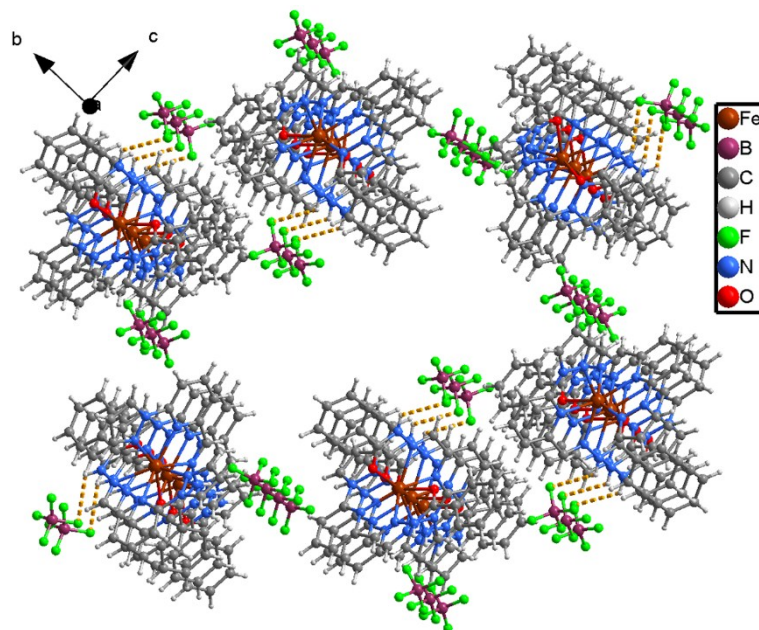


Fig. S6. The π - π packing diagram and hydrogen bonding network in **compound 2**

Table S4. Hydrogen bond distances (Å) and bond angles (°) for **pypzbeyz·CH₃OH**

D-H...A	d(D-H)	d(H...A)	d(D...A)	∠(DHA)
N(5)-H(5)...O(2)	0.86	2.06	2.877(3)	159.1
O(2)-H(2A)...O(1)#1	0.82	2.00	2.802(3)	165.7

Symmetry code: #1 x-1, y, z

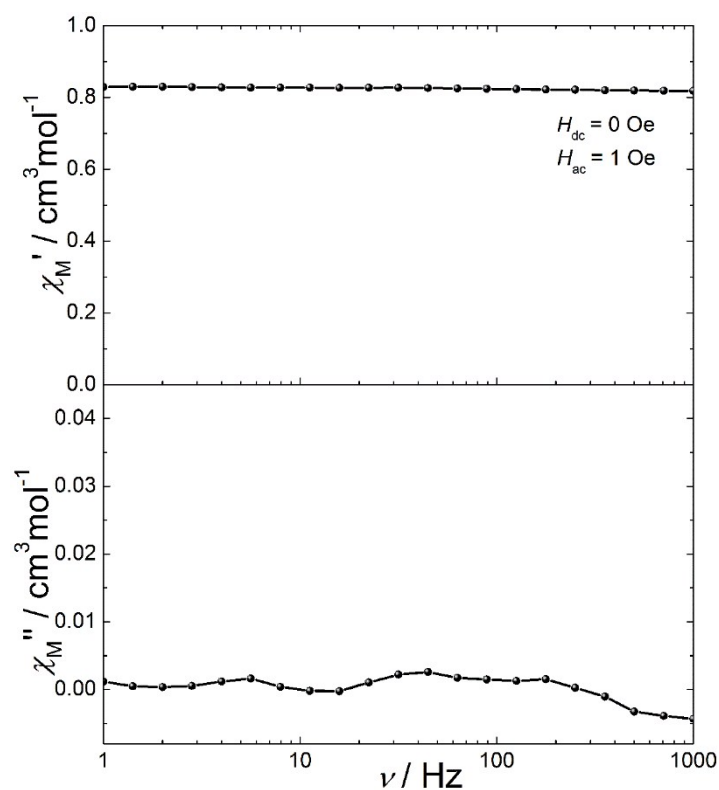
Table S5. Hydrogen bond distances (Å) and bond angles (°) for **1**

D-H...A	d(D-H)	d(H...A)	d(D...A)	∠(DHA)
N(5)-H(5)...O(5)#1	0.86	2.52	3.134(3)	128.7
N(5)-H(5)...O(7)#1	0.86	2.15	2.961(3)	156.9

Symmetry code: #1 -x+1,-y+1,-z+1

Table S6. Hydrogen bond distances (Å) and bond angles (°) for **2**

D-H...A	d(D-H)	d(H...A)	d(D...A)	∠(DHA)
N(5)-H(5)...F(2)	0.86	2.07	2.881(4)	157.1
N(10)-H(10)...F(5)	0.86	2.00	2.825(4)	161.1

**Fig. S7.** Frequency dependence of the in-phase (χ_M') and out-of phase (χ_M'') ac susceptibilities for **1** at 2 K under a Zero Oe dc field from 1 Hz to 999 Hz.

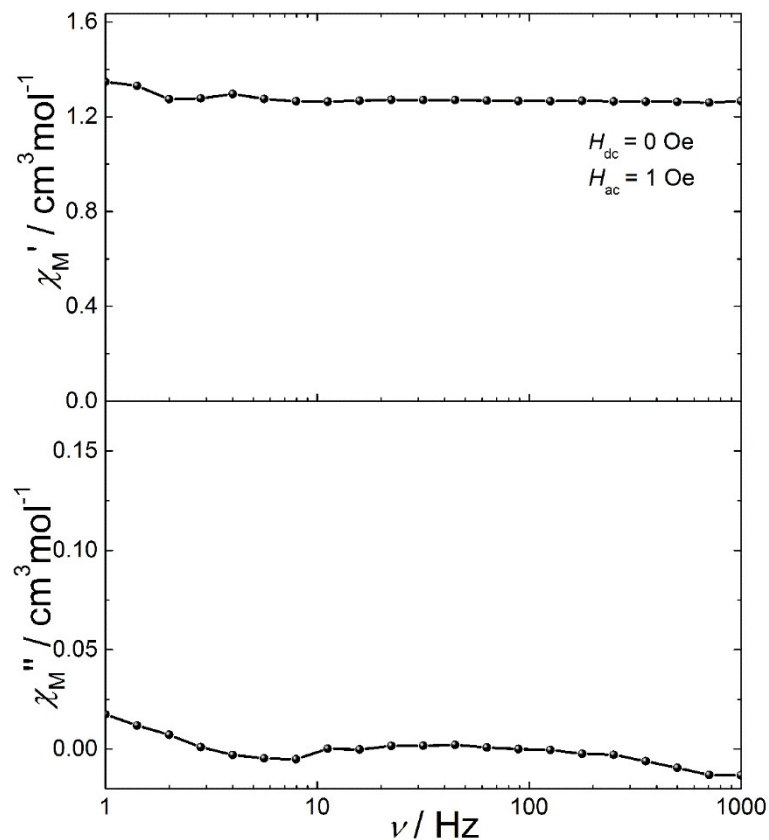


Fig. S8. Frequency dependence of the in-phase (χ_M') and out-of phase (χ_M'') ac susceptibilities for **2** at 2 K under a Zero Oe dc field from 1 Hz to 999 Hz.

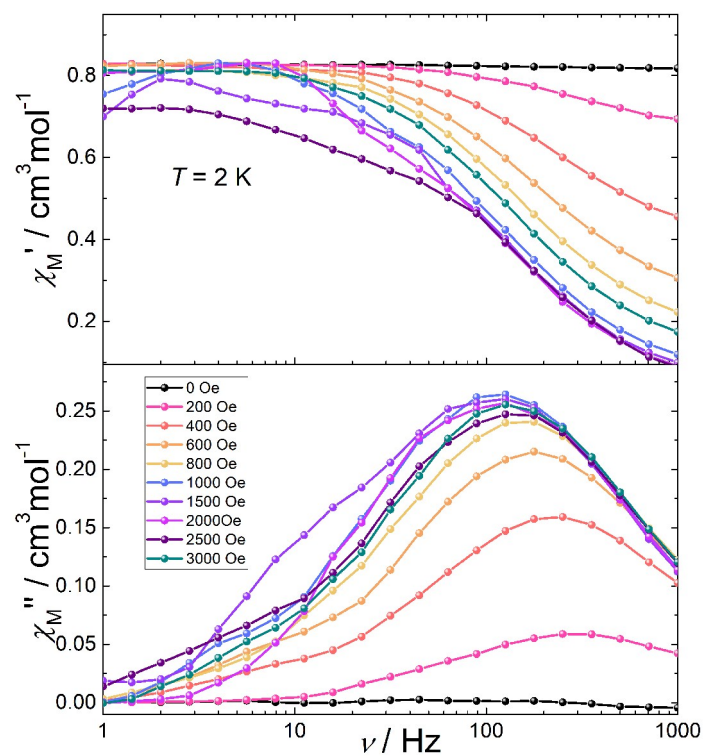


Fig. S9. Frequency dependence of the in-phase (χ_M') and out-of phase (χ_M'') ac susceptibilities measured under various applied dc fields (0–3000 Oe) at 2 K for compound **1**.

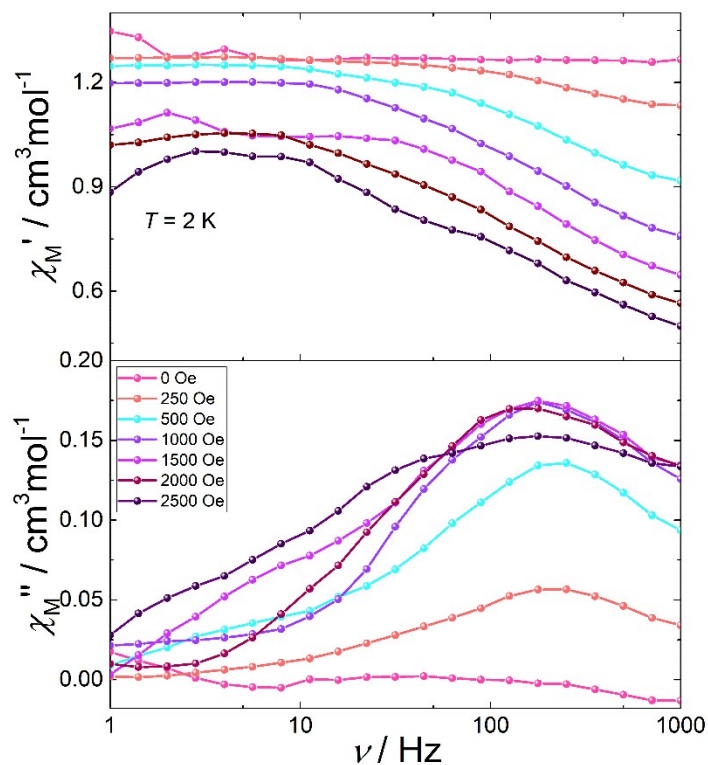


Fig. S10. Frequency dependence of the in-phase (χ_M') and out-of phase (χ_M'') ac susceptibilities measured under various applied dc fields at 2 K for compound **2**.

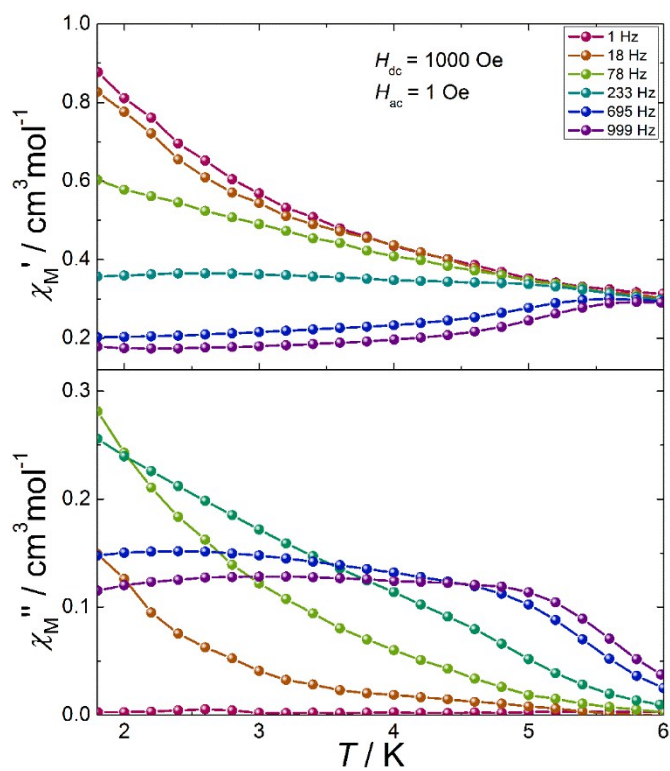


Fig. S11. Temperature dependence of the in-phase (χ_M') and out-of phase (χ_M'') ac susceptibilities for **1** under a 1000 Oe dc field.

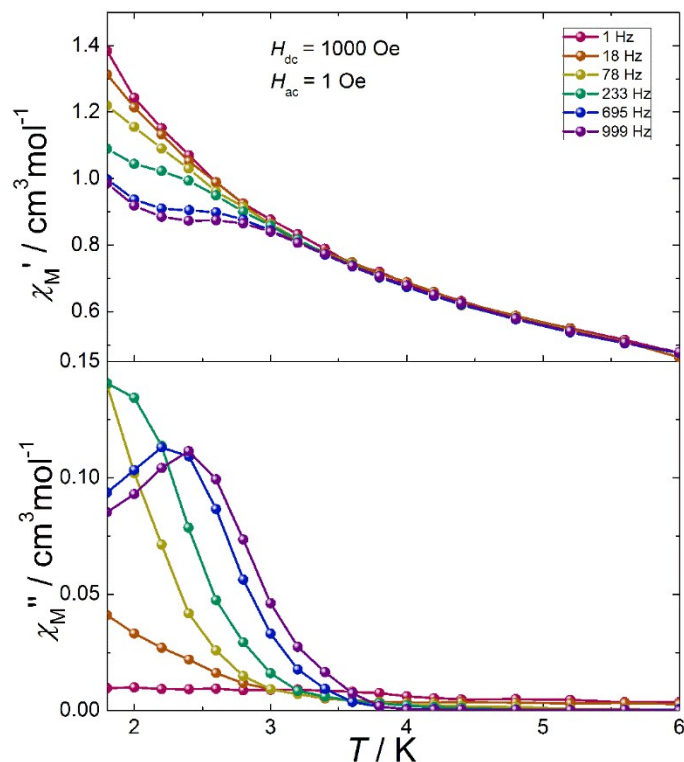


Fig. S12. Temperature dependence of the in-phase (χ_M') and out-of phase (χ_M'') ac susceptibilities for **2** under a 1000 Oe dc field.

Table S7. Relaxation Fitting Parameters from the Least-Square Fitting of the Cole-Cole plots of compound **1** according to the Generalized Debye Model

Temperature / K	$\chi_S / \text{cm}^3 \text{mol}^{-1} \text{K}$	$\chi_T / \text{cm}^3 \text{mol}^{-1} \text{K}$	τ / s	α
1.8	0.11442	0.89000	0.00144	0.17772
2.0	0.09460	0.83324	0.00127	0.21924
2.2	0.09270	0.75291	0.00102	0.20718
2.4	0.09597	0.68334	8.5E-4	0.18617
2.6	0.08000	0.65984	7.8E-4	0.22156
2.8	0.07940	0.61192	6.6E-4	0.21626
3.0	0.07974	0.56138	5.6E-4	0.19799
3.2	0.07000	0.53226	4.7E-4	0.19805
3.4	0.08000	0.50801	4.4E-4	0.18751
3.6	0.07998	0.48045	3.9E-4	0.18675
3.8	0.07000	0.45687	3.4E-4	0.19555
4.0	0.08000	0.43840	3.1E-4	0.17407
4.2	0.07999	0.41255	2.6E-4	0.15399
4.4	0.08000	0.39603	2.3E-4	0.14187
4.6	0.08000	0.38310	1.9E-4	0.14052
4.8	0.07925	0.36615	1.6E-4	0.12000
5.0	0.07998	0.35083	1.2E-4	0.08888
5.2	0.06996	0.34079	9E-5	0.09463

5.4	0.07000	0.32770	7E-5	0.06342
5.6	0.05421	0.31783	5E-5	0.06345

Table S8. Relaxation Fitting Parameters from the Least-Square Fitting of the Cole-Cole plots of compound **2** according to the Generalized Debye Model

Temperature / K	$\chi_S / \text{cm}^3\text{mol}^{-1}\text{K}$	$\chi_T / \text{cm}^3\text{mol}^{-1}\text{K}$	τ / s	α
1.8	0.91799	1.34583	0.00112	0.24757
2.0	0.82419	1.24250	6.8E-4	0.30056
2.2	0.73593	1.15349	3.2E-4	0.33246
2.4	0.59593	1.07680	1.1E-4	0.44714
2.6	0.49837	0.98748	3E-5	0.40503